OFFICE OF NAVAL RESEARCH

GRANT or CONTRACT: N00014-93-1-0772

R & T Code 313T006

Technical Report #11

Solution and Solid C^{13} NMR Studies of Polyolacrylate Networks

Lungu,A.; Neckers, D. C. *J. Coatings Research* **1995** in press. (invited paper: graduate student award).

DTIC
ELECTE
JUL 1 3 1995
S D
F

D. C. Neckers
Center for Photochemical Sciences
Dept. of Chemistry
Bowling Green State University
Bowling Green, OHIO 43402

Date Submitted
June 15, 1995

Reproduction in whole, or in part, is permitted for any purpose of the United States Government.

This document has been approved for public release and sale, its distribution is unlimited.

19950705 070

DTIC QUALITY INSPECTED 5

REPORT DOCUMENTATION PAGE

Form Approved OMB No. 0704-0188

Public reporting burden for this collection of information is estimated to average 1 hour per response, including the time for reviewing instructions, searching existing data sources, gathering and maintaining the data needed, and completing and reviewing the collection of information. Send comments regarding this burden estimate or any other aspect of this collection of information, including suggestions for reducing this burden, to Washington Headquarters Services, Directorate for Information Operations and Reports, 1215 Jefferson Davis Highway, Suite 1204, Arlington, VA 22202-4302, and to the Office of Management and Budget, Paperwork Reduction Project (0704-0188), Washington, DC 20503

1. AGENCY USE ONLY (Leave blank)

2. REPORT DATE
6-15-95

3. REPORT TYPE AND DATES COVERED
Technical Report

4. TITLE AND SUBTITLE
Solution and Solid C^{13} NMR Studies of Polyolacrylate Networks

5. FUNDING NUMBERS
G N00014-93-J-1921
R & T 313T006

6. AUTHOR(S)
D.C. Neckers

Kenneth Wynne

7. PERFORMING ORGANIZATION NAME(S) AND ADDRESS(ES)
Center for Photochemical Sciences
Bowling Green State University
Bowling Green, Ohio 43402

8. PERFORMING ORGANIZATION REPORT NUMBER
11

9. SPONSORING/MONITORING AGENCY NAME(S) AND ADDRESS(ES)
Department of the Navy
Office of Naval Research
800North Quincy Street
Arlington, VA 22217-5000

10. SPONSORING/MONITORING AGENCY REPORT NUMBER

11. SUPPLEMENTARY NOTES
Lungu,A.; Neckers, D. C. *J. Coatings Research* **1995** in press. (invited paper: graduate student award).

12a. DISTRIBUTION/AVAILABILITY STATEMENT
Reproduction in whole or in part is permitted for any purpose of the United States Government. This document has been approved for public release and sale; its distribution is unlimited.

12b. DISTRIBUTION CODE

13. ABSTRACT (Maximum 200 words)

We introduce the use of several C13 NMR techniques to address the problem of the structures of photopolymerized polyolacrylates. We have used these techniques to study both the liquid and solid states of acrylic monomers and oligomers, and the network structure formed upon their photopolymerization. High resolution NMR has allowed us to consider the molecular structure of the acrylic groups belonging to each of a series of polyolacrylate monomers. In photopolymerization experiments, by measuring the relative intensity of specific peaks in the carbon spectra as a function of time of irradiation and laser power, it is possible to determine the relative reactivity of monomers/oligomers used in the early stages of polymerization. By monitoring the variation of the proton T1ρ relaxation time, changes in the cross-link density, and in the mobility of the polymeric chains, can be followed throughout the photopolymerization process. The degree of crosslinking is correlated to the relaxation times and increases with an increasing power of the irradiating laser even under conditions where the degree of conversion, as measured by quantitative infrared absorption of the 810 cm-1 band of the acrylate is unchanged.

14. SUBJECT TERMS

15. NUMBER OF PAGE

16. PRICE CODE

17. SECURITY CLASSIFICATION OF REPORT	18. SECURITY CLASSIFICATION OF THIS PAGE	19. SECURITY CLASSIFICATION OF ABSTRACT	20. LIMITATION OF ABS
Unclassified	Unclassified	Unclassified	UL

NSN 7540-01-280-5500

Standard Form 298 (Rev. 2-89)
Prescribed by ANSI Std. Z39-18
298-102

Solution and Solid C^{13} NMR Studies of Polyolacrylate Networks

by

Adrian Lungu and D. C. Neckers*
Center for Photochemical Sciences†
Bowling Green State University
Bowling Green, OHIO 43402

Accesion For	
NTIS CRA&I	☑
DTIC TAB	☐
Unannounced	☐
Justification	
By	
Distribution /	
Availability Codes	
Dist	Avail and / or Special
A-1	

Abstract:

Most photopolymerizable coating materials employed in various applications throughout industry are comprised of crosslinkable polyolacrylates. On a molecular level, these systems are difficult to characterize when polymerized mainly because they are insoluble and intractable. Just a few techniques provide fundamental structural information or can be used to characterize the dynamic features of these complex, cross-linked gels.

We introduce the use of several C13 NMR techniques to address the problem of the structures of photopolymerized polyolacrylates. We have used these techniques to study both the liquid and solid states of acrylic monomers and oligomers, and the network structure formed upon their photopolymerization. High resolution NMR has allowed us to consider the molecular structure of the acrylic groups belonging to each of a series of polyolacrylate monomers. In photopolymerization experiments, by measuring the relative intensity of specific peaks in the carbon spectra as a function of time of irradiation and laser power, it is possible to determine the relative reactivity of

† Contribution # from the Center for Photochemical Sciences

monomers/oligomers used in the early stages of polymerization. By monitoring the variation of the proton T1ρ relaxation time, changes in the cross-link density, and in the mobility of the polymeric chains, can be followed throughout the photopolymerization process. The degree of crosslinking is correlated to the relaxation times and increases with an increasing power of the irradiating laser even under conditions where the degree of conversion, as measured by quantitative infrared absorption of the 810 cm^{-1} band of the acrylate is unchanged.

INTRODUCTION

Coatings such as those widely used in various industrial radiation polymerized systems often consist of crosslinked polymer networks which are mainly polyolacrylates. The introduction of polyolacrylates for the formation of clear polymers rapidly formed by exposure to UV light in the presence of certain small molecule photoinitiators traces to Plambeck, at DuPont, who developed them for use in preparing relief images for printing plates. According to a critical Plambeck patent 'one of the most widely used photoengraving processes at the time (1956) was to expose metals coated with very thin layers of gelatins photosensitive to light through an image bearing transparency thus forming a reverse image in the photosensitive layers ...'.[1] Plambeck's seminal contribution was to recognize that multifunctionality in an acrylate would produce a more rapid photoresponse and that benzoin ethers absorbed radiation at the principle lines of the mercury resonance lamp, underwent radical forming reactions which we now know to be of the Norrish Type I series, and thereby formed photopolymers which were clear and colorless. Plambeck's work built on an earlier British patent[2] which taught that relief-forms for printing could be produced from methyl methacrylate, the primary monomer for the formation of Plexiglas® in an image forming manner which also often required a subsequent thermal forming step. In a typical DuPont system, various polyolacrylates were photopolymerized with the examples cited including on polyethylene glycol diacrylate, and various polyolacrylates formed from glycerol, pentaerythritol, triethylene glycol, and so on. Among the many characteristics of photopolymers formed from such materials are their clarity and hardness. Such materials also

undergo very rapid photopolymerizations, a point stressed as being important in printing applications by Plambeck.

Polyolacrylate monomers when polymerized, today have many other applications. For example, they provide the shiny coats in thin films such as those found on the cover of magazines like National Geographic. Among other applications of these monomers are as printing inks, for coatings, in lithography, for three dimensional imaging/stereolithography, and for near photographic speed color copying systems such as Cycolor®[3] . The actual number of monomers used in such applications now includes several hundreds. Among the more common are highly functionalized examples such as trimethylolpropane triacrylate and dipentaerythritol pentaaacrylate, Figure 1.

As critical as polyolacrylates are in commerce,[4] very little actual structural information on the photopolymers formed from them is available. This is in direct contrast to the photopolymerized systems created by crosslinking of poly(vinyl cinnamates) developed by Minsk, van Deusen and Robertson at Eastman Kodak[5] the photoproducts from which have been characterized completely and in detail by Reiser in a series of now classic works in photopolymer science.[6] There are several reasons for this. First, photopolyolacrylates are commercial and they work for the purposes for which they were intended. Much of the impetus for further development has now passed to formulating companies the staffs of which have different motivations than the basic science of the systems with which they are working. Second, unraveling the structures of such highly functionalized polymers is a difficult task at best - impossible at worst. Before the use of the techniques we report herein, actual structural studies would have been impossible.

For several years, we have been concerned with understanding the relationship between the photochemistry and photophysics of initiators and

coinitiators used to form photopolymers and the mechanical properties of the materials which form from them. The reason for this is that much of the impetus for the use of photopolymerization methods in imaging processes has passed to three dimensional systems, and a direct implication of this is the potential for the photoformation of functional objects by stereolithography. We have become interested in developing photopolymer systems which produce objects which can be directly used as functional parts. It therefore becomes critical to develop methods to establish the actual chemical structures of highly functionalized poly(polyolacrylates), as well as to sort out the specific reactivity of all of the acrylate double bonds in each of the monomers, and we have undertaken that task.

Understanding the molecular structure of formed polymer networks is a complex problem because the many processes which occur in the formation of photopolymers from polyolacrylates do not always go to completion and the reactions by which they are formed sometimes continue for long periods of time. For example, it is not unusual for the various processes occuring during a photopolymerization reaction to start in the nanosecond time domain after light absorption, and to continue in time frames ranging from many minutes to many hours. Both early occuring and late occuring polymerization processes can impact on photopolymer properties. Nevertheless, the individual reactions can be followed independently by a combination of solution phase and solid C13 nmr spectroscopy, and that is what we describe below.

What has been lacking in this work to date is reliable structural information about polymer structure. The information content of a DSC or photo DSC plot, as important as that can be, is limited because DSC measures a

colligative property - the heat of polymerization. Infrared measurements, for example of the disappearance of acrylate functionality, give fingerprint information about an assembly of carbon-carbon double bonds. As useful as infrared spectroscopy is, in the case of polymerized polyolacrylates, the method is unable to distinguish one double bond from another. Since many of the mixtures used in coatings applications contain 10 or more individual acrylate double bonds as part of three or more individual monomers, this is a particular disadvantage. Photoformed polymeric polyolacrylates are difficult to characterize mainly because they are essentially insoluble. Analytical techniques such as like GPC and spectroscopic techniques requiring solutions cannot be used in the determination of their structure.

Since an understanding of the molecular structure of photoformed polyolacrylates is critical in order to understand and affect the final properties of the materials formed from them, we have recently undertaken structural studies of complex network polymers by solution and solid state nmr. Among the various structural characteristics of these materials we anticipate nmr will help understand are how the crosslinking density relates to the diffusion rate of a solvent or monomer through the formed polymers, to their hardness, and to other physical properties[7]. We also anticipate that by determining the relative reactivity of individual monomers those who develop formulations for the many applications in which the systems are used may be guided in the choice of new monomer/oligomers to be used for specific applications.

Since the polymers in question are generally insoluble and intractable, NMR stands as one of the most useful techniques for providing in-depth information about molecular structure. It can be used in the liquid and in the solid state, thus allowing the analysis of both monomer/oligomer and the final cross-linked polymer[8]. It can be applied to the various elements of polymeric systems, for example carbon, hydrogen and silicon. Besides providing static structural information, NMR also allows the determination of parameters related to the polymer dynamics like the T_1 and $T_{1\rho}$ parameters. These values are anticipated to provide an in-depth evaluation of the dynamic behavior of specific atoms or groups of atoms, and the extent of their interactions with their immediate environment[9,10].

We have used C13 NMR, both in the liquid and solid state in order to determine various structural parameters of monomer mixtures and their photopolymerized networks. Among the parameters studied are the average degree of polymerization of the acrylate monomer/oligomers employed, the relative reactivity of each one of the monomers in the mixture, $T_{1\rho}$ relaxation times of carbon atoms, and the variation of the cross-linked density with the laser power. We have specifically concentrated on a general formulation of polyolacrylates.

EXPERIMENTAL

General:

An Ar+ laser (Omnichrome 543-200 MGS) was used as the radiation source. Carbon-13 NMR spectra for the liquids were obtained at room temperature using a Varian Gemini 200 spectrometer operating at 50.3 MHz. A Varian UnityPlus 400 spectrometer operating at 100.6 MHz was used for the solid samples.

The monomers and oligomers used (Figure 1) were: a) Polyethylene glycol-400, diacrylated, [PEGA-400] (from Monomer-Polymer Laboratories, Inc.); b) Butyl acrylate, [BuAc] (Aldrich Chem. Co.); c) 1,6-Hexanediol diacrylate, [HDDA] (Aldrich Chem. Co.); d) Trimethylolpropane triacrylate, [TMPTA], (Sartomer 357, from Sartomer Co.); e) Dipentaerythritol pentaacrylate, [DPHPA], (Sartomer 399, from Sartomer Co.); f) the monomer mixture, STDR, consisted of, in weight percent, PEGA (20), TMPTA (40), DPHPA (40). Monomer stabilizers were not removed because it has been observed that doing so generates an instability in the reaction mixture, and the polymerization starting before it is really intended.

The dye used as photoinitiator was a fluorone derivative (2,4-diiodo-6-butoxy-3 fluorone) hereafter DIBF[11] at concentrations which varied from $2x10^{-4}$ M to $1x10^{-3}$ M. N,N-dimethyl-2,6-diisopropylaniline, [DIDMA], (from Carbolabs, Inc.), was used as the electron donor with at concentrations varying from $3x10^{-3}$ M to 0.1 M.

Sample Preparation:

The monomers and the mixtures of monomers were dissolved in *d*-chloroform for the liquid phase nmr determinations. For the relative reactivity measurements the irradiation was carried out directly in an NMR tube. The laser power was varied from 10 mW to 70 mW, and the scan speed was 11.0 mm/sec.

For the solid-state experiments the reactive mixture was poured into dogbone-shaped Teflon molds. The laser beam was directed toward the sample by mirrors positioned above the molds. The mirrors were controlled by *x-y* scanners (DX-series servo controller, from General Scanning, Inc.) driven by digitized computer data from a special file which traced over a bit more than a 200.0 x 200.0 mm square region. This is large enough to cover the entire dog-bone-shaped mold.. The laser power was varied from 40 mW to 150 mW, and the scan speed was 9.0 mm/sec[1].

After the irradiation was complete, the photopolymerized dog-bones were immersed in liquid nitrogen and crushed. Silicon nitride rotors were filled with the sample's powder and the samples were spun at the magic angle with a spinning rate of 7.0 kHz at 290° K.

RESULTS AND DISCUSSION

1. Liquid Phase

Relative Reactivity

The C13 NMR spectra of BuAc, HDDA, PEGA, TMPTA, and DPHPA are shown in Figures 2a-e. Since the carbon atoms of the acrylic double bonds for each monomer have specific chemical shifts, one may follow the reactivity of these monomers in homogeneous solution and their relative reactivity in mixtures. HDDA was mixed with each monomer in different proportions (1:1 by weight with PEGA, TMPTA, DPHPA, and 1:3 with BuAc) and the changes in the intensity of the peaks corresponding to carbon-carbon double bonds as a function of laser power measured. DIBF [$2x10^{-4}$ M] was used in combination with co-initiator [$3x10^{-3}$ M] in every case. The results, Figure 3, compare the intensity of the methylene carbon resonance of the acrylic double bond of each monomer (BuAc, PEGA, TMPTA, DPHPA) with that of the methylene carbon

resonance of the acrylic double bonds from HDDA. As Figure 3a suggests, by increasing the laser power, the relative intensity of the peak corresponding to the C13 resonance of the acrylic double bonds in PEGA to that of the similar C13 resonance in HDDA decreases. This indicates that PEGA is more reactive than HDDA under these polymerization conditions. The variation in relative C13 resonance intensity of the peaks corresponding to the methylene carbons in the acrylic double bonds of HDDA:BuAc with laser power for the mixture HDDA:BuAc is given in Figure 3b. It is observed that the change in relative intensity is bigger when the laser power is incremented from 0 to 30 mW. At higher power levels, the relative reactivity remains almost constant. This suggests that BuAc is only slightly less reactive than HDDA since the concentration of BuAc is controlled in such a way such that there are 3 acrylic groups in the BuAc system for the two acrylic groups of HDDA.

For mixtures of DPHPA:HDDA and TMPTA:HDDA a different behavior is observed. At laser powers from 10 to 30 mW, the relative intensity of the C13 resonances of the $-CH_2$ carbons increases in both cases, suggesting that HDDA is more reactive than either DPHPA or TMPTA, Figures 3c,d. If the laser power is increased beyond 30 mW, the relative intensity of the C13 resonances of the methylene carbons of the acrylic groups decreases. In the case of DPHPA the intensity of this resonance drops from 1.26 at 30 mW to 0.68 at 40 mW, Figure 3c. Data were obtained up to a laser power of 50 mW beyond which the mixture changed to a gel rendering the NMR technique inaccurate. After a certain, specific laser powers, it appears that DPHPA and TMPTA become more reactive than HDDA. At laser powers lower than the threshold value, HDDA is more likely to react than DPHPA and TMPTA. We presume this is due to the differences in molecular weight and relative molecular size since radicals from it would be expected to be more mobile in solution. When the number of DPHPA

and TMPTA radicals formed reach this threshold value (by increasing the laser power, more radicals are produced), the photopolymerization of these two multifunctional monomers (DPHPA has 5 acrylic groups and TMPTA has 3 acrylic groups) becomes very fast.

The following relative reactivity order can be established from the data in Figure 3: DPHPA > TMPTA > PEGA >HDDA = BuAc. DPHPA is the most reactive, due to its five acrylic groups, and BuAc the least reactive.

By measuring the distances between the peaks in the C13 NMR spectra corresponding to the CH_2 and CH of the acrylic double bonds in each monomer, and by matching these distances in the mixture, all the peaks could be identified as shown in Figure 4.

The increase in relative C13 intensity for each monomer could be monitored during the photopolymerization process by measuring the intensity of the C-O peak relative to the intensity of the CH_2 peak from the double bond carbon system. This gives a measure of relative reactivity. These experiments were carried out on two separate samples; DIBF = [1.0×10^{-3} M]; DIDMA = [1.5×10^{-2} M]. The experiments were done as follows: the to-be-polymerized mixture was introduced, respectively, into two NMR tubes and dissolved in $CDCl_3$. One sample, [sample B] was kept in room light after having been irradiated at a laser power of 30 mW. As expected, the relative intensity (the ratio between the intensity of the C-O peak and the intensity of the CH_2 peak from the acrylic double bond) increased with time for all of the monomers, Figure 5a-c. After 1.5 hr the mixture became a gel and no more determinations were possible. The second sample [sample C] was kept in the dark after irradiation. All monomers behaved in a similar manner, Figures 6a-c. In the first four hours after irradiation, the relative intensity of C-O peak too that of the CH_2 increased rapidly. After that the increase was much slower. For example, in the case of

PEGA the ratio increased from 4.15 to 4.47 in the first 4 hours and after that from 4.47 to 5.2 in a 68 hour period. In the case of TMPTA, the ratio increased from 1.99 to 2.09 in the first 4 hours, and from 2.09 to 2.21 during the rest of the experiment. In the case of DPHPA the same ratio increased from 2.32 to 2.51 in the beginning and from 2.51 to 2.8 during the remaining 68 hours of the experiment. These results suggest that, even for the sample kept in the dark, polymerization continues even after the laser is turned off because of the presence of radicals formed in the early stages of the polymerization process.

After the double bond conversion reaches a value of 4-5%, liquid becomes gel, and the sample no longer remains soluble in $CDCl_3$. Therefore, to follow the photopolymerization process after the early stages, one must use solid-state C13 NMR.

2. Solid-state studies

Mobility

Matched spin-lock (SL), single-contact cross-polarization (CP), or Hartmann-Hahn experiments were performed using a four part procedure. First, the proton spins were polarized in H_0. Then they were placed in the rotating frame by a 90° pulse followed by a 90° phase shift and continuous application of a strong H1 rf field. The third part of the experiment was to establish C13-H1 contact for variable times by placing the C13 spins into the rotating frame by continuous rf irradiation of the carbon spins such that $\gamma_{carbon}(H_1)_{carbon}=\gamma_{proton}(H_1)_{proton}$. The final step was to sample the C13 magnetization by turning off $(H_1)_{carbon}$, but still with dipolar decoupling of the H1 spins[12].

The buildup of carbon magnetization as a function of spin-lock CP contact with polarized protons is shown for the STDR (20% PEGA, 40% TMPTA, 40%

DPHPA) in Figure 7. The polymerized sample was obtained with a laser power of 100 mW, and these spectra were taken with magic-angle spinning. The mixture contained some residual monomer, and not every double bond was converted to a single bond. The peak assignments for the mixture, from Figure 8, are made from the spectra of the monomer in solution, are: 175 ppm for the carbonyl group of the nonpolymerized acrylic groups, 165 ppm for the carbonyl group of the polymer, 131 ppm for the CH_2 carbon of the residual acrylic double bonds, 128 ppm for the CH carbon from the residual acrylic double bonds, 70 ppm for the CH_2-O carbons from DPHPA and PEGA, 64 ppm for the CH_2-O carbon from TMPTA, 45 ppm for the quaternary carbon from DPHPA, 41 ppm for the quaternary carbon from TMPTA, 24 ppm for the -CH- carbon from the polymerized acrylate double bonds, 18 ppm for the -CH_2- carbon from the polymerized acrylate double bonds, and 7.5 ppm for the methyl carbon of TMPTA. The difference between the carbon resonances of the C=O group in the nonpolymerized acrylic groups and the carbon resonances of the carbonyl group of the polymer is due to the loss of conjugation in the second case. This causes a downfield chemical shift of about 9-10 ppm.

After about 4 ms of CP contact, the intensity of all the carbon lines decreases, Figure 7. The time constant describing this decay is the proton $T_{1\rho}$, which can be correlated with the motions of protonated carbon atoms in the polymeric network. The mobility of these carbons depends on the degree of crosslinking as well. Large values for proton $T_{1\rho}$ means the carbon atom has substantial mobility and a relatively low degree of crosslinking. Six different samples were studied at different values of the contact time (from 0.2 ms to 10 ms). The photoreactive mixture was photopolymerized with six different laser powers (40 mW, 60 mW, 80 mW, 100 mW, 120 mW, and 150 mW) but with the

scan speed maintained. The initiator, DIBF [$3x10^{-3}$ M] and DIDMA [0.1 M] served as the initiating system.

Figure 9a-e presents the variation of the proton $T_{1\rho}$ with laser power for each protonated carbon. In every case, we observed an increase in the proton $T_{1\rho}$ with an increase of laser power from 40 mW to approximately 80 mW, and a decrease in proton $T_{1\rho}$ at higher laser powers. This implies that the mobility of the carbon atoms are increasing with laser power until the mobility reaches a maximum around 80 mW. After that carbon atom mobility is decreasing. This can be explained if one assumes that the degree of crosslinking is low at reduced laser power and each of the carbons have sufficient space to move about in the polymeric network. An increase in the laser power causes an increase in the degree of crosslinking, and the polymer chains become tighter and tighter. This limits the mobility of the individual carbon atoms. This causes a decrease in the $T_{1\rho}$ values. As was determined from the IR spectra, the C=C conversion does not increase significantly with an increase in laser power over 80 mW, but the degree of crosslinking still appears to increase. The % C=C conversion was determined by squeezing a few drops of resin between NaCl windows separated with 1.5 mm Teflon spacers. The IR transmission spectrum was measured before irradiation. The sample was then irradiated and the FTIR transmission spectrum taken again. The % C=C was determined by comparing the area of the 810 cm^{-1} absorption peak of the acrylic group before and after irradiation and using the equation:

$$\% \, C{=}C = (S_0 - S_1) \times 100 / S_0 \qquad (1)$$

where S_0 corresponds to the area of the band before irradiation and S_1 is the area after irradiation[7]. A comparison between the double bond conversion and the degree of crosslinking is presented in Figure 10.

The variation of the chemical shift of the methyl carbon from TMPTA with the laser power is presented in Figure 11. With an increase in the laser power from 40 mW to 80 mW, this peak is shifted downfield. An additional increase in power causes the peak to shift in the reverse direction, or upfield. This peak shift is due to the fact that at small laser powers (no more than 80 mW) individual carbon atoms have significant mobility, as was pointed out above, and the CH_3 carbon atom are able to be significantly separated from the acrylic groups. As a result, steric interactions are reduced. At higher laser power (above 80 mW) such mobility decreases due to the increase in the crosslink density. The methyl carbon is this system is closer to the network matrix and the peak shifts upfield. A shift downfield is also due to the fact that the electron density decreases around the CH_3 carbon[13] (higher mobility in the network increases the space between the C=O and CH_3 groups).

CONCLUSIONS

C13 NMR in liquid and solid state is proving to be a most useful technique for the characterization of polyolacrylate networks. The relative reactivity between the components of most complex mixtures as a function of laser power may be determined by following the variation of the intensity ratio of the carbon resonance of C-O carbon atom and the carbon resonance of CH_2 carbon derived from the acrylic double bonds. The disadvantage of the solution method is that such monitoring can be carried out only until 5% percent of the double bonds are converted to single bond centers. At higher values of double bond conversion the polymers formed are insoluble in the required nmr solvents such as chloroform.

By following the variation of the relaxation times of individual carbon resonances as a function of laser power, information concerning the mobility of specific groups in the polymer can be obtained. For example, carbons from the

residual acrylic double bonds have greater mobility than the corresponding carbons from the polymerized double bonds. The CH_2-O carbons have less mobility than the CH_2 and CH carbons from the polymeric chain, and the value of $T_{1\rho}$ does not change appreciabliy with laser power. The CH_2 carbons from the polymerized acrylic double bonds and the CH_3 carbons appear to have comparable mobility by using this analysis.

In the particular system studied in this work (an acrylic network), the degree of crosslinking continues to increase above 100 mW laser power though variations in the degree of double bond conversion are very small. We have also found that the degree of crosslinking can be correlated with the chemical shift of the CH_3 carbon of the TMPTA.

A combination of solution phase and solid state C13 nmr studies promise important new information about the three dimensional structures of polymer networks. Our work is continuing.

ACKNOWLEDGEMENT:

This work has been supported by the National Science Foundation (NSF : DMR-9013109) and the Navy Office of Research (N00014-93-1-0772). We are most grateful for the support of these agencies. We also acknowledge, with gratitude, discussions with Dr. Afranio Torres-Filho of these laboratories.

REFERENCES:

[1] L. F. Plamback, Jr. U. S. Patent 2,760,863. August 28, 1956; *et. seq.* to E. I. DuPont de Nemours and Company, Wilmington, Del.
[2] Gates, British Patent 566,795. January 15, 1945.
[3] P. Gottschalk, D.C. Neckers, and G.B. Schuster, U.S. Patent #4,772,530, E.P. # 90201194.9; P. Gottschalk, P. D. Davis and G. B. Schuster, U. S. Patent, 4,772,541,

September, 1988; P. Adair, P. Gottschalk, D. C. Neckers, G. B. Schuster and S. P. Pappas, U. S. Patent #4,977,511 (December 11, 1990).

[4] Current estimates indicate the markets for all photopolymerization technologies worldwide are about $1,000,000,000/annually.

[5] L. M. Minsk, W. P. van Deusen, and E. M. Robertson, U. S. Patent # 2,610,120, September 9, 1952

[6] A. Reiser, "

[7] Torres-Filho, A., Neckers, D. C., *Journal of Applied Polymer Science*, **51**, 931 (1994).

[8] Le Menestrel, C., Kenwright, A. M., Sergot, P., Laupretre, F., Monnerie, L., *Macromolecules*, **25**, 3020 (1992).

[9] Kalachandra, S., Turner, D. T., Burgess, J. P., Stejskal, E. O., *Macromolecules*, **27**, 5948 (1994).

[10] Schantz, S., Ljungqvist, N., *Macromolecules*, **26**, 6517 (1993).

[11] Tanabe, T., Torres-Filho, A., Neckers, D. C., *Journal of Polymer Science; Polymer Chemistry Ed.*, (in press).

[12] Schaefer, J., Stejskal, E. O., Buchdahl, R., *Macromolecules*, **10**, 384 (1977).

[13] Li, S., Chesnut, D. B., *Magnetic Resonance In Chemistry*, **23**, 625 (1985).

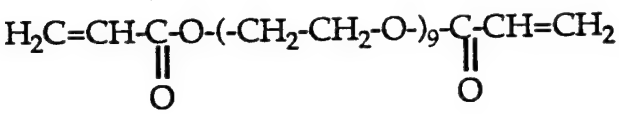

PEGA-400

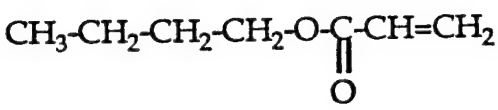

BuAc

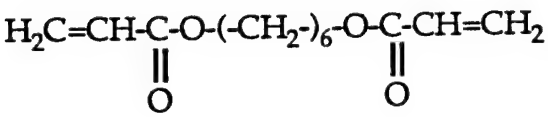

HDDA

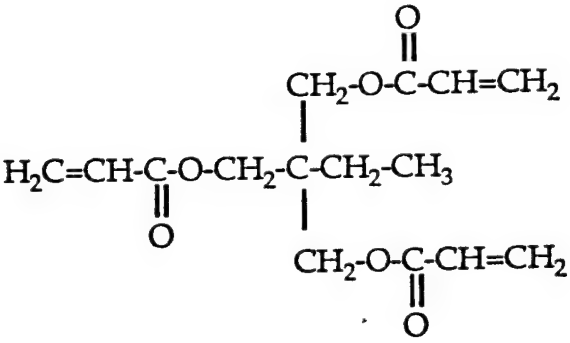

TMPTA

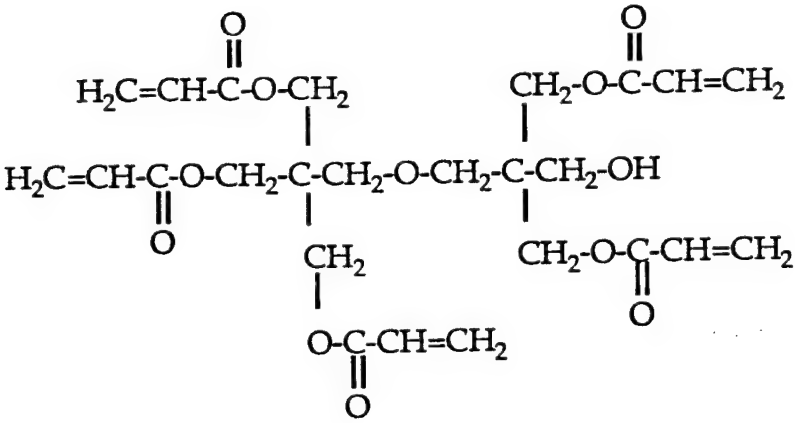

DPHPA

Fig. 1.

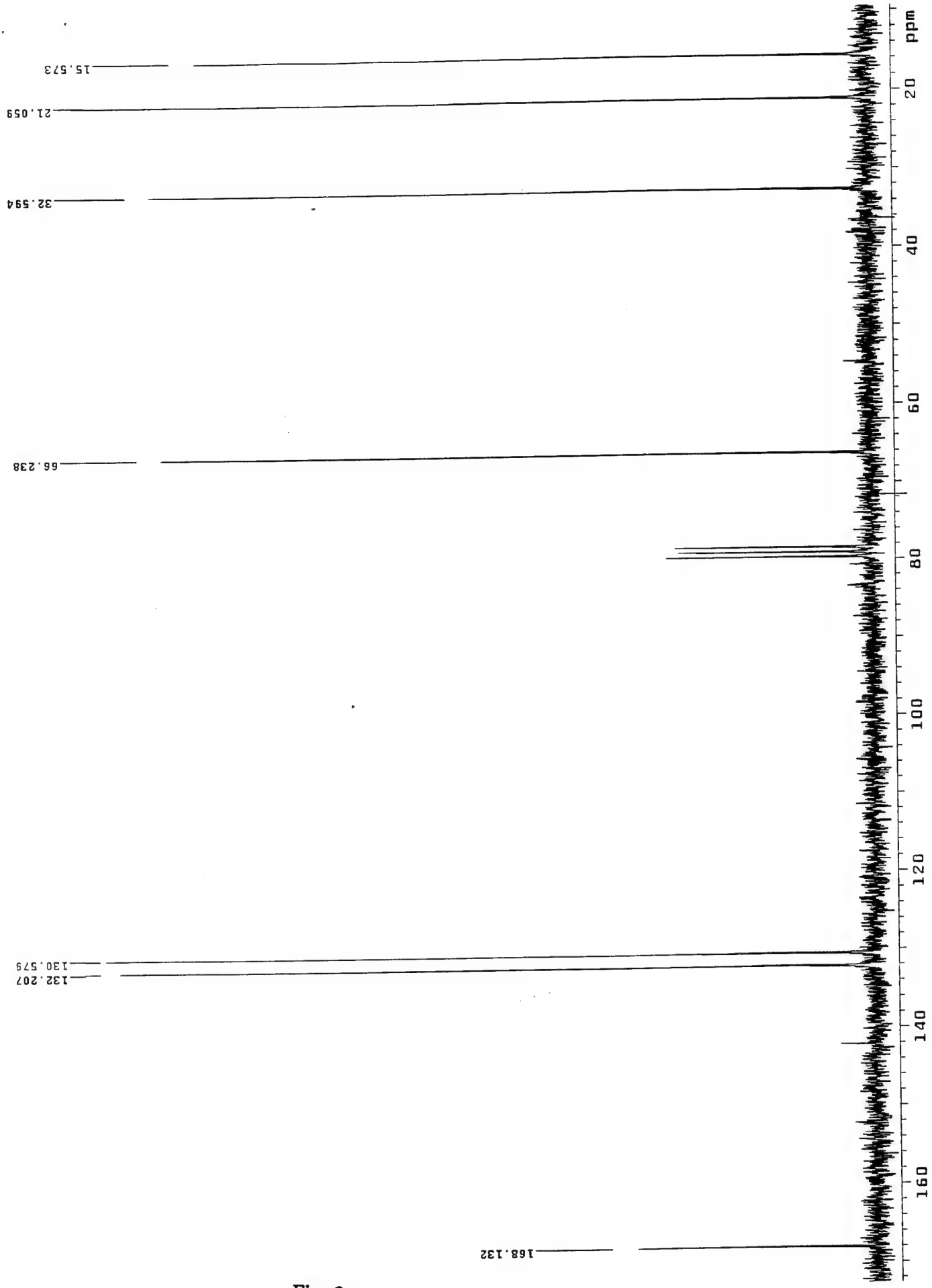
168.132
132.207
130.579
66.238
32.594
21.059
15.573
ppm
160
140
120
100
80
60
40
20

Fig. 2a.

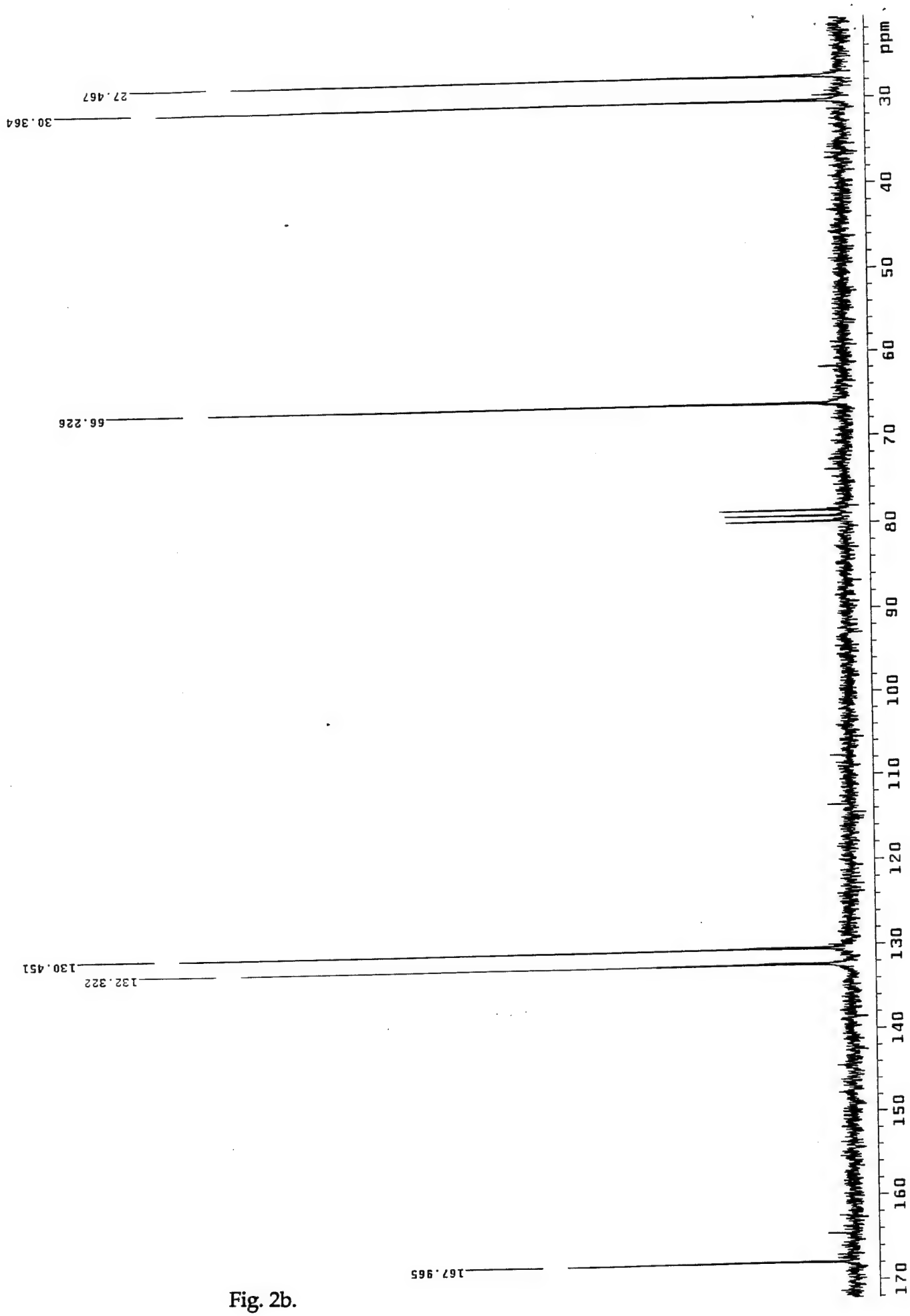
27.467
30.364
66.226
130.451
132.322
167.965
ppm
30
40
50
60
70
80
90
100
110
120
130
140
150
160
170

Fig. 2b.

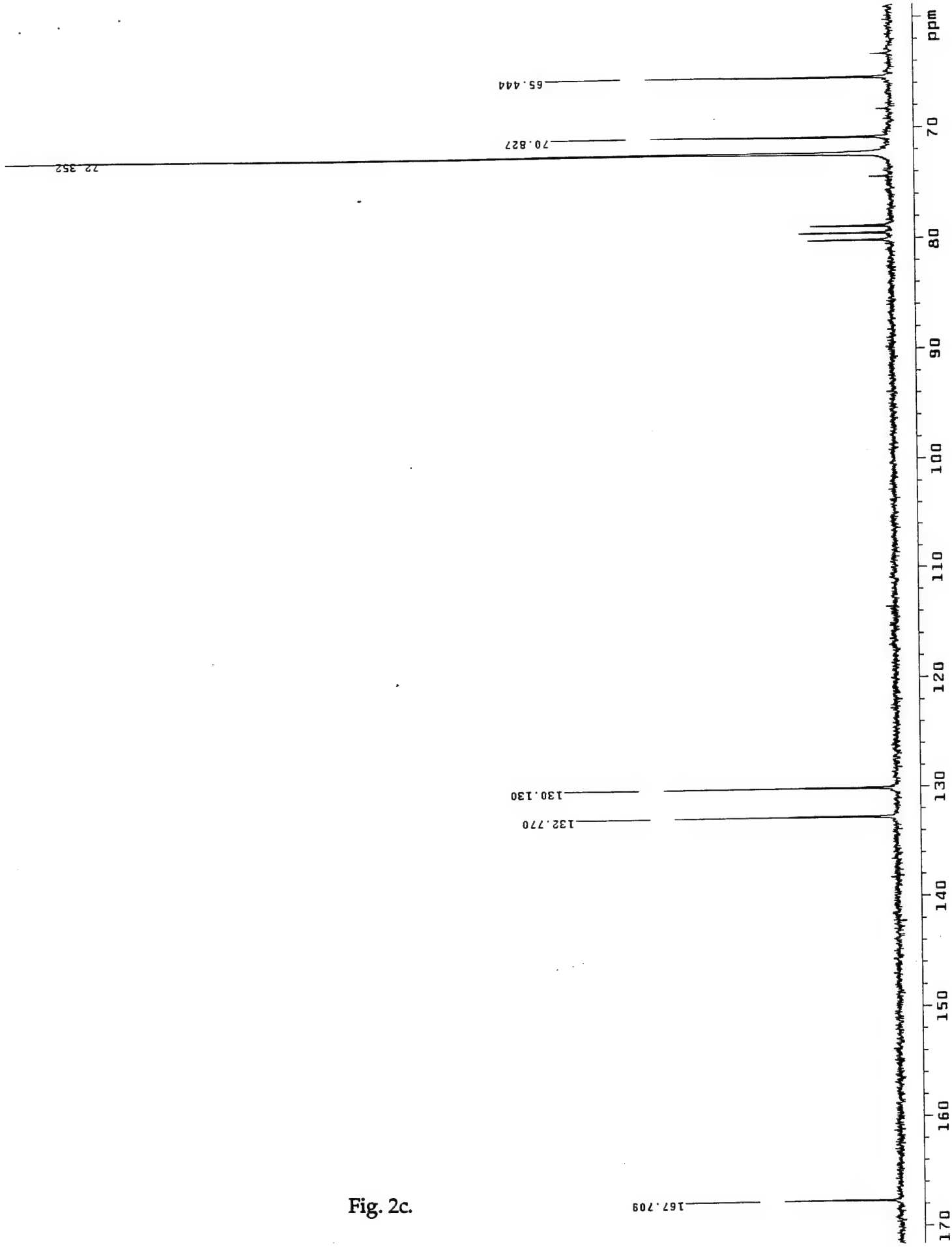
ppm
70
80
90
100
110
120
130
140
150
160
170
65.444
70.827
22.352
130.130
132.770
167.709

Fig. 2c.

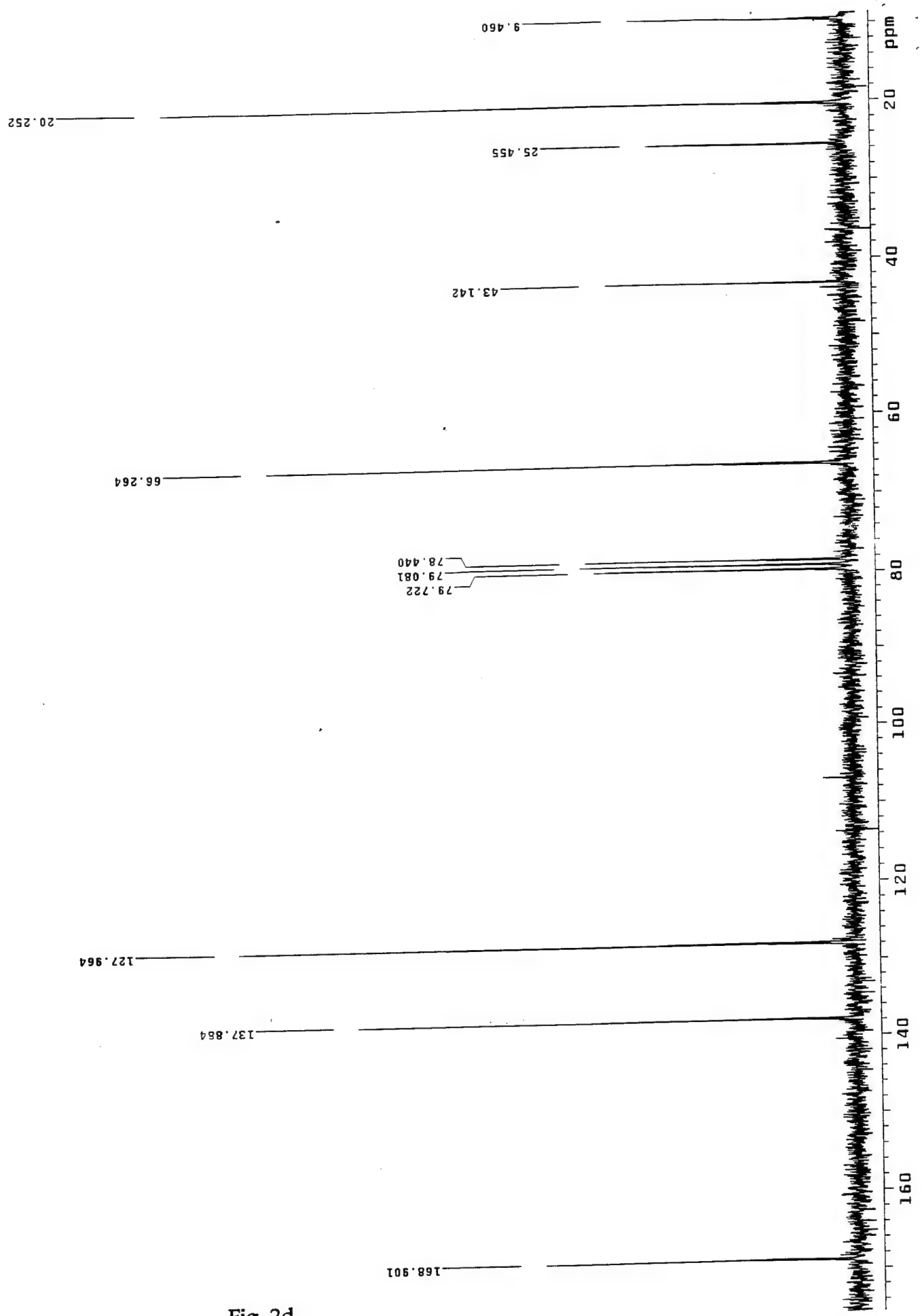
168.901
137.854
127.964
79.722
79.081
78.440
66.264
43.142
25.455
20.252
9.460
ppm
160
140
120
100
80
60
40
20

Fig. 2d.

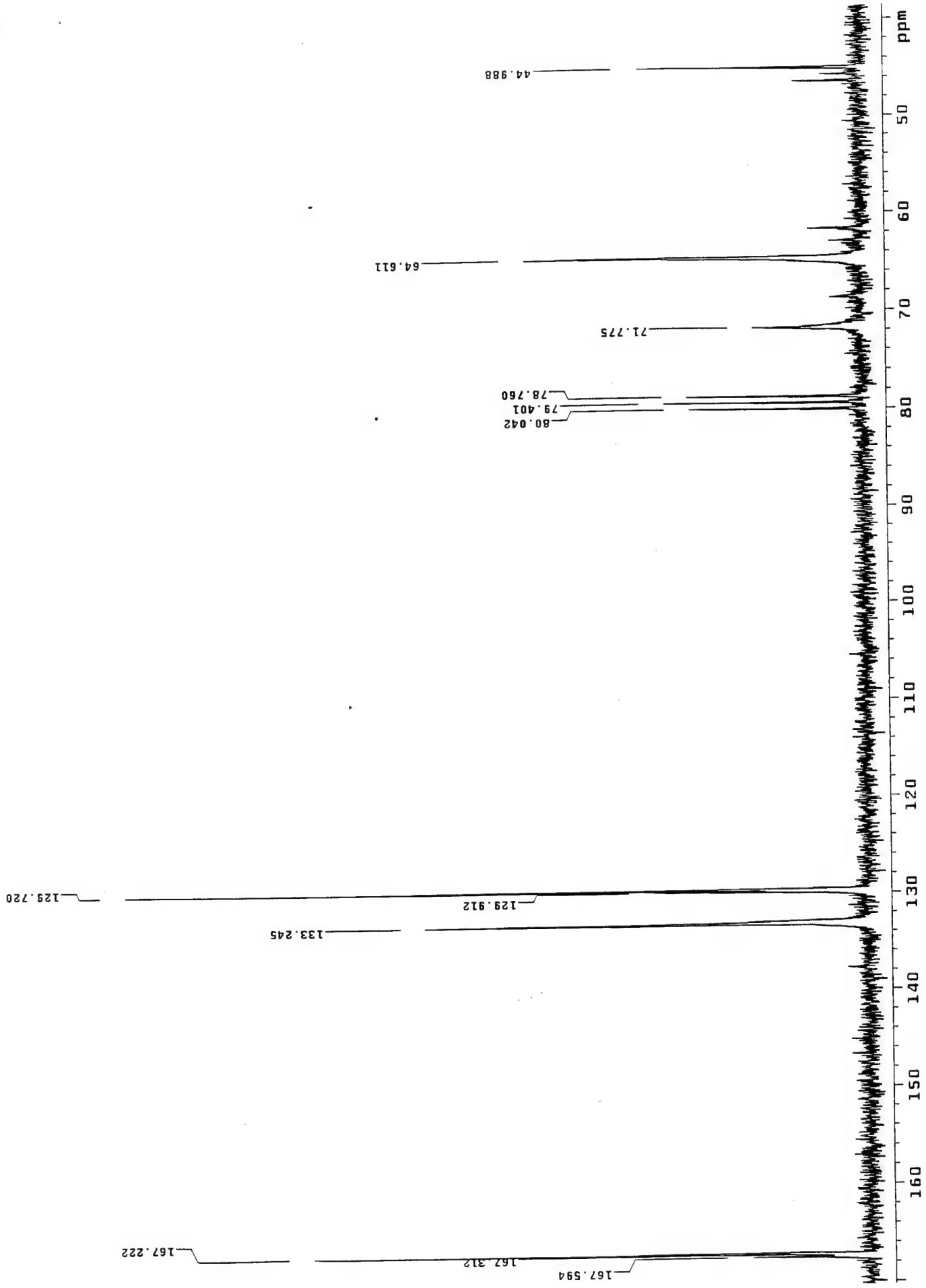
ppm
50
60
70
80
90
100
110
120
130
140
150
160
44.988
64.611
71.775
78.760
79.401
80.042
129.912
129.720
133.245
167.594
167.312
167.222

Fig. 2e.

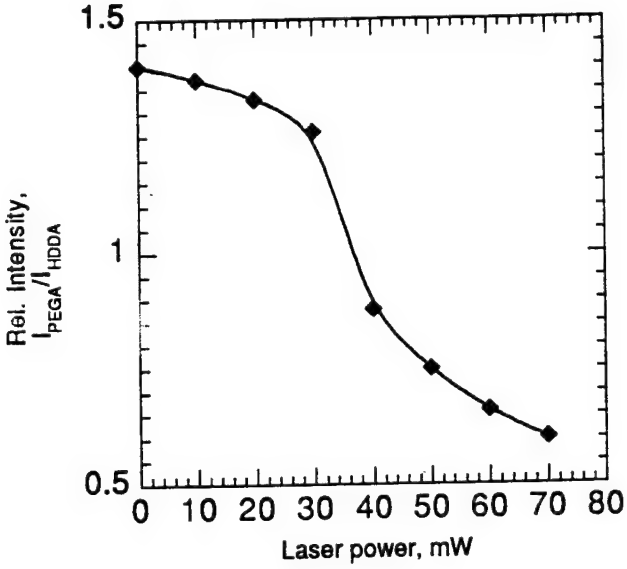
1.5
1
0.5
Rel. Intensity,
I_{PEGA}/I_{HDDA}
0 10 20 30 40 50 60 70 80
Laser power, mW

Fig. 3a.

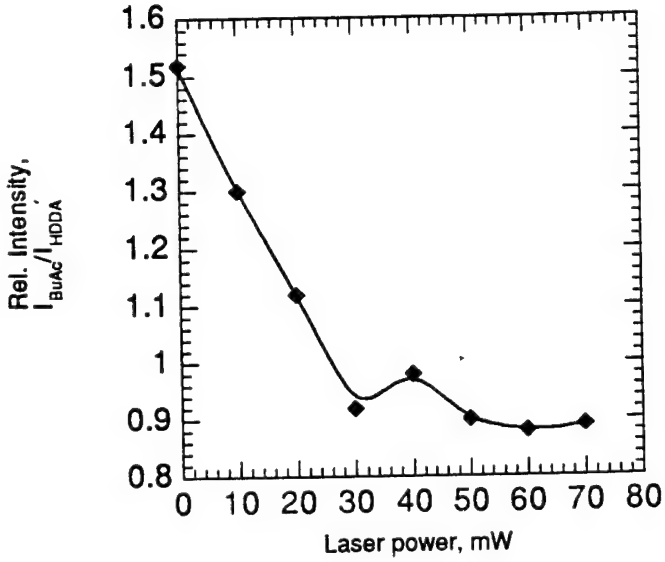
1.6
1.5
1.4
1.3
1.2
1.1
1
0.9
0.8
Rel. Intensity,
I_{BuAc}/I_{HDDA}
0 10 20 30 40 50 60 70 80
Laser power, mW

Fig. 3b.

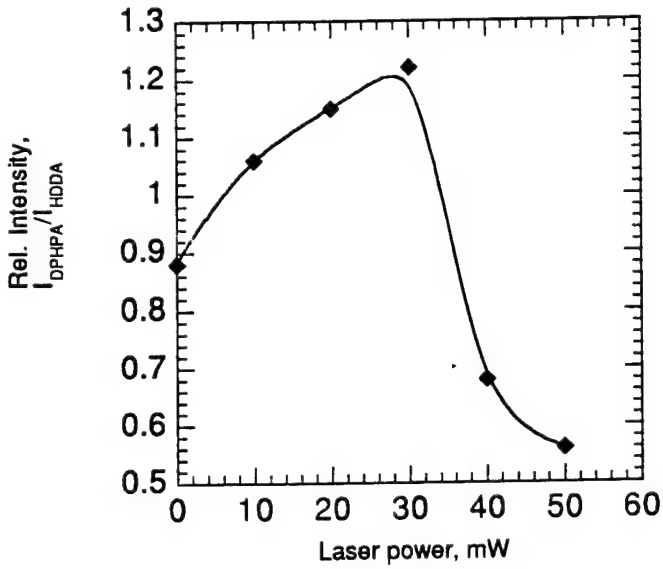
1.3
1.2
1.1
1
0.9
0.8
0.7
0.6
0.5
Rel. Intensity,
I_{DPHPA}/I_{HDDA}
0
10
20
30
40
50
60
Laser power, mW

Fig. 3c.

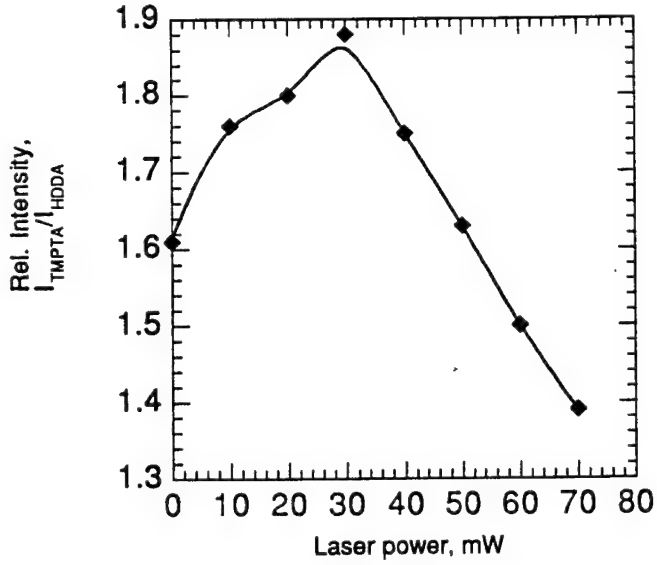
1.9
1.8
1.7
1.6
1.5
1.4
1.3
Rel. Intensity,
I_{TMPTA}/I_{HDDA}
0 10 20 30 40 50 60 70 80
Laser power, mW

Fig. 3d.

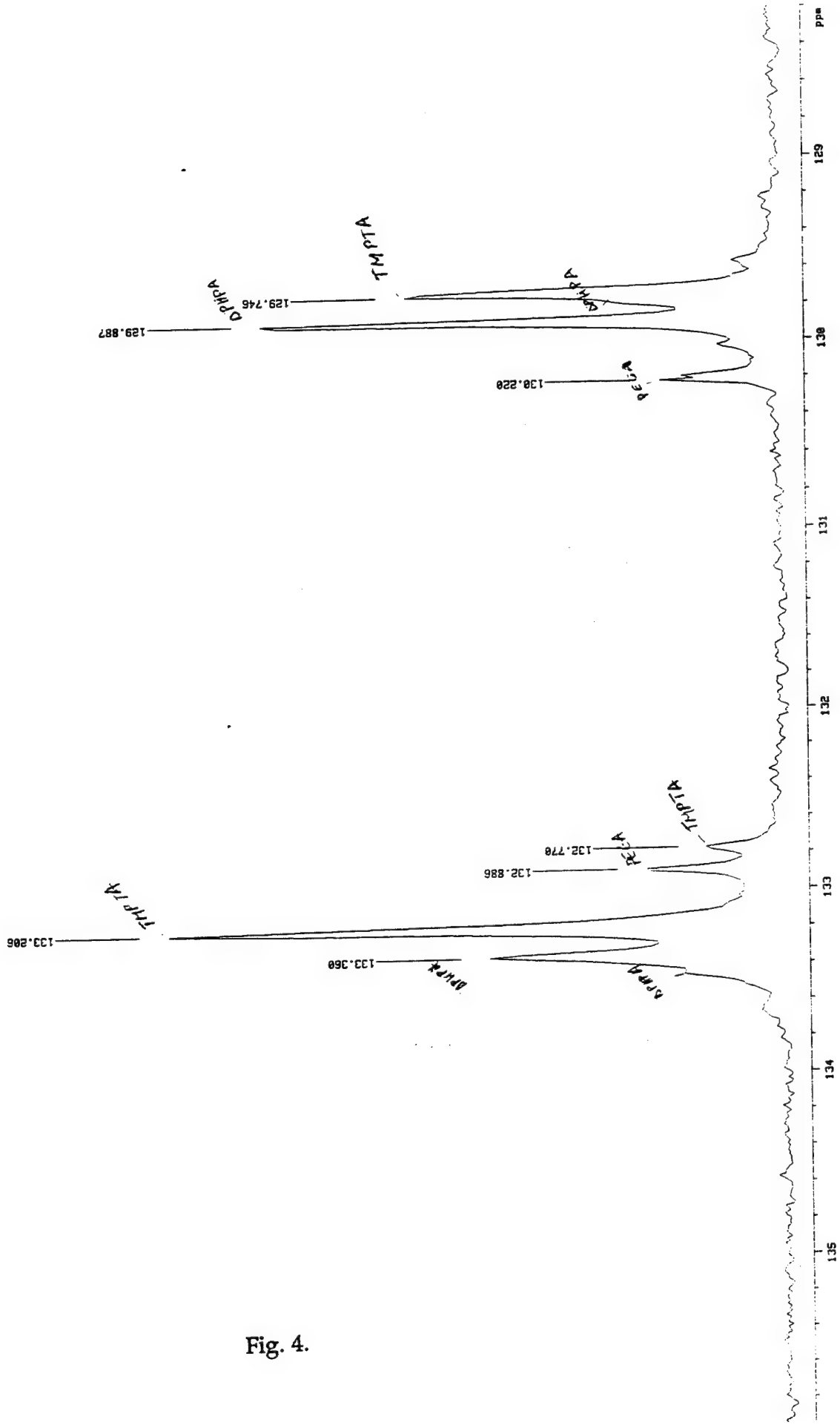
ppm
129
130
131
132
133
134
135
129.887
129.746
130.220
132.770
132.886
133.206
133.360
DPHPA
TMPTA
DPHPA
PEGA
TMPTA
PEGA
TMPTA
DPHPA
DPHPA

Fig. 4.

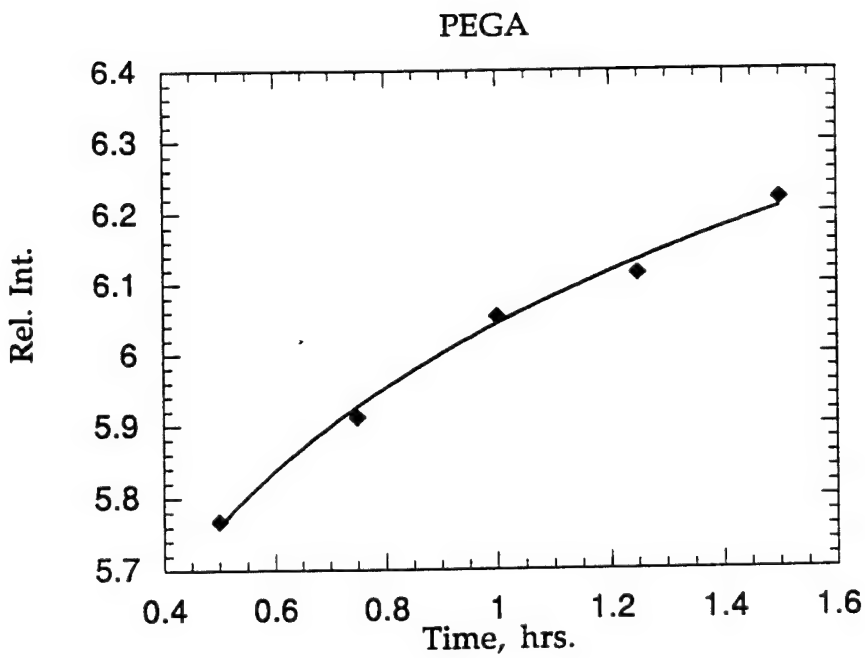

Fig. 5a.

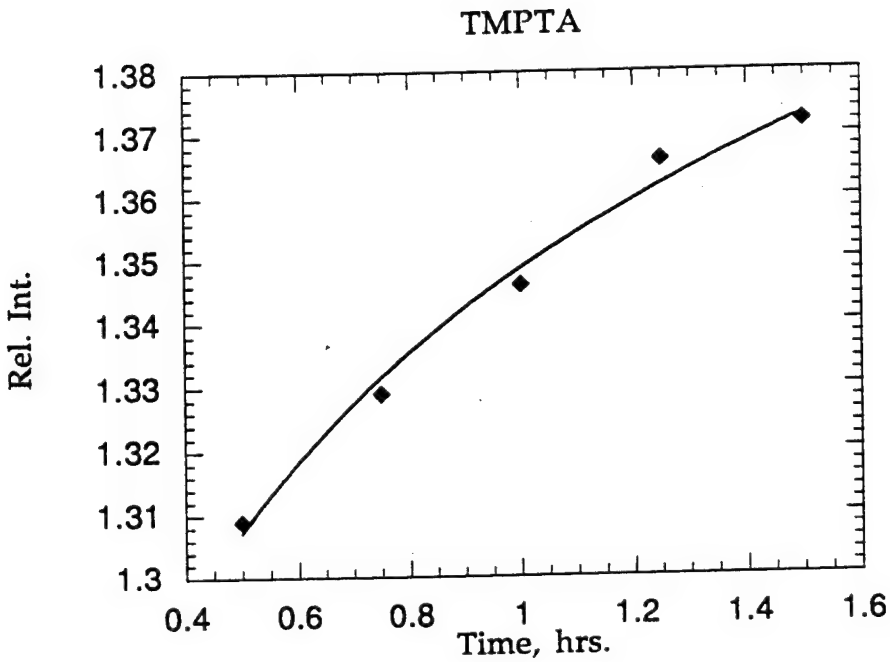
TMPTA
1.38
1.37
1.36
1.35
1.34
1.33
1.32
1.31
1.3
Rel. Int.
0.4
0.6
0.8
1
1.2
1.4
1.6
Time, hrs.

Fig. 5b.

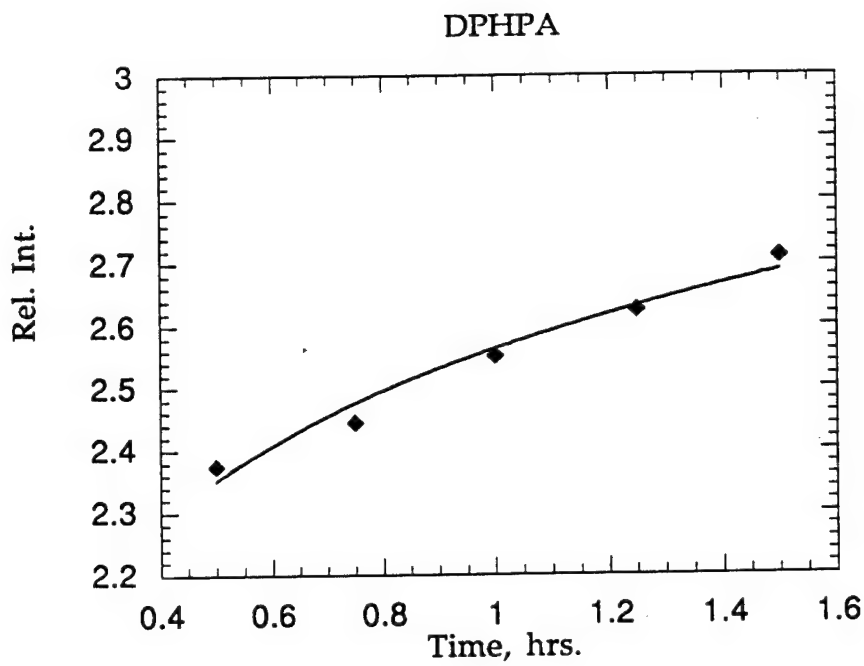

Fig. 5c.

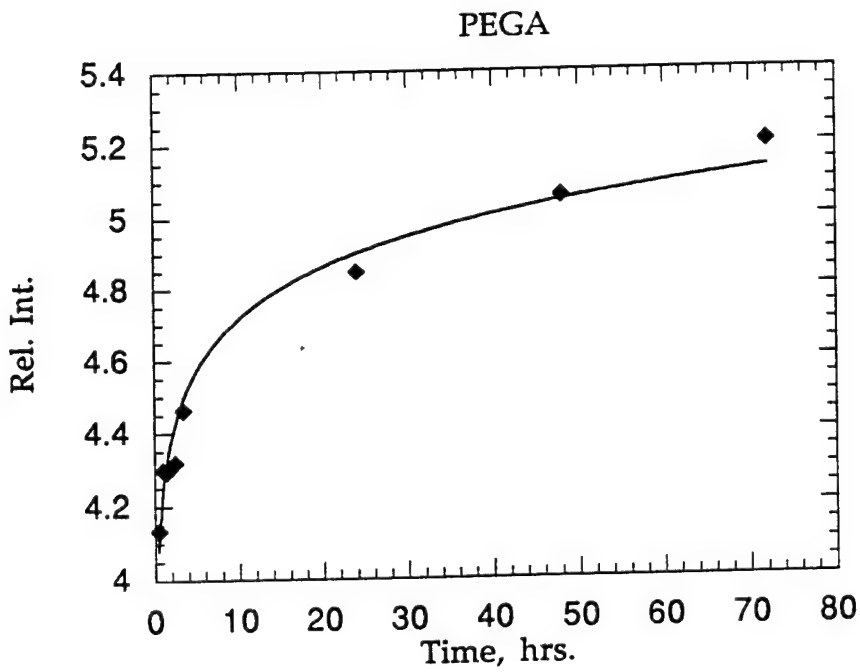

Fig. 6a.

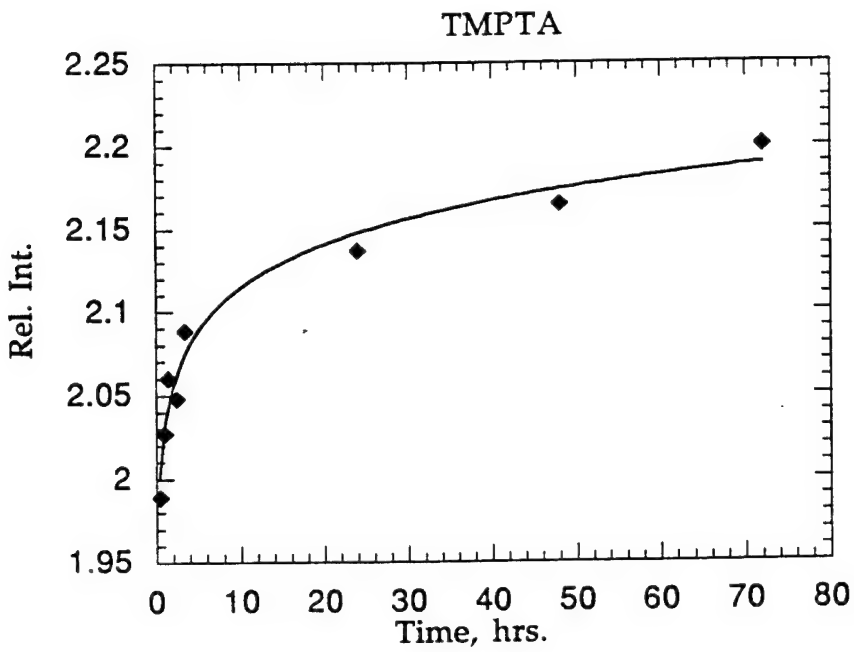
TMPTA
2.25
2.2
2.15
2.1
2.05
2
1.95
Rel. Int.
0
10
20
30
40
50
60
70
80
Time, hrs.

Fig. 6b.

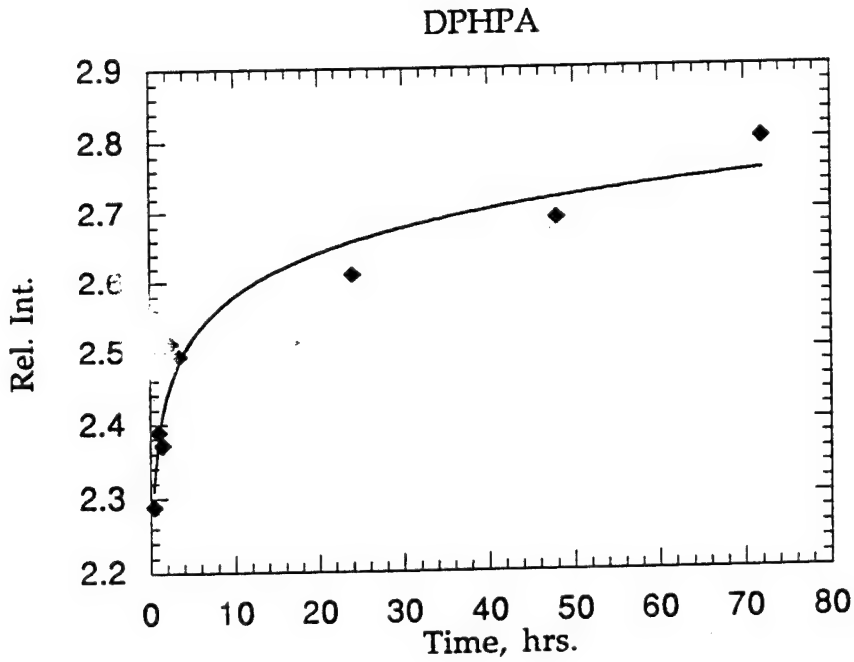
DPHPA
2.9
2.8
2.7
2.6
2.5
2.4
2.3
2.2
Rel. Int.
0
10
20
30
40
50
60
70
80
Time, hrs.

Fig. 6c.

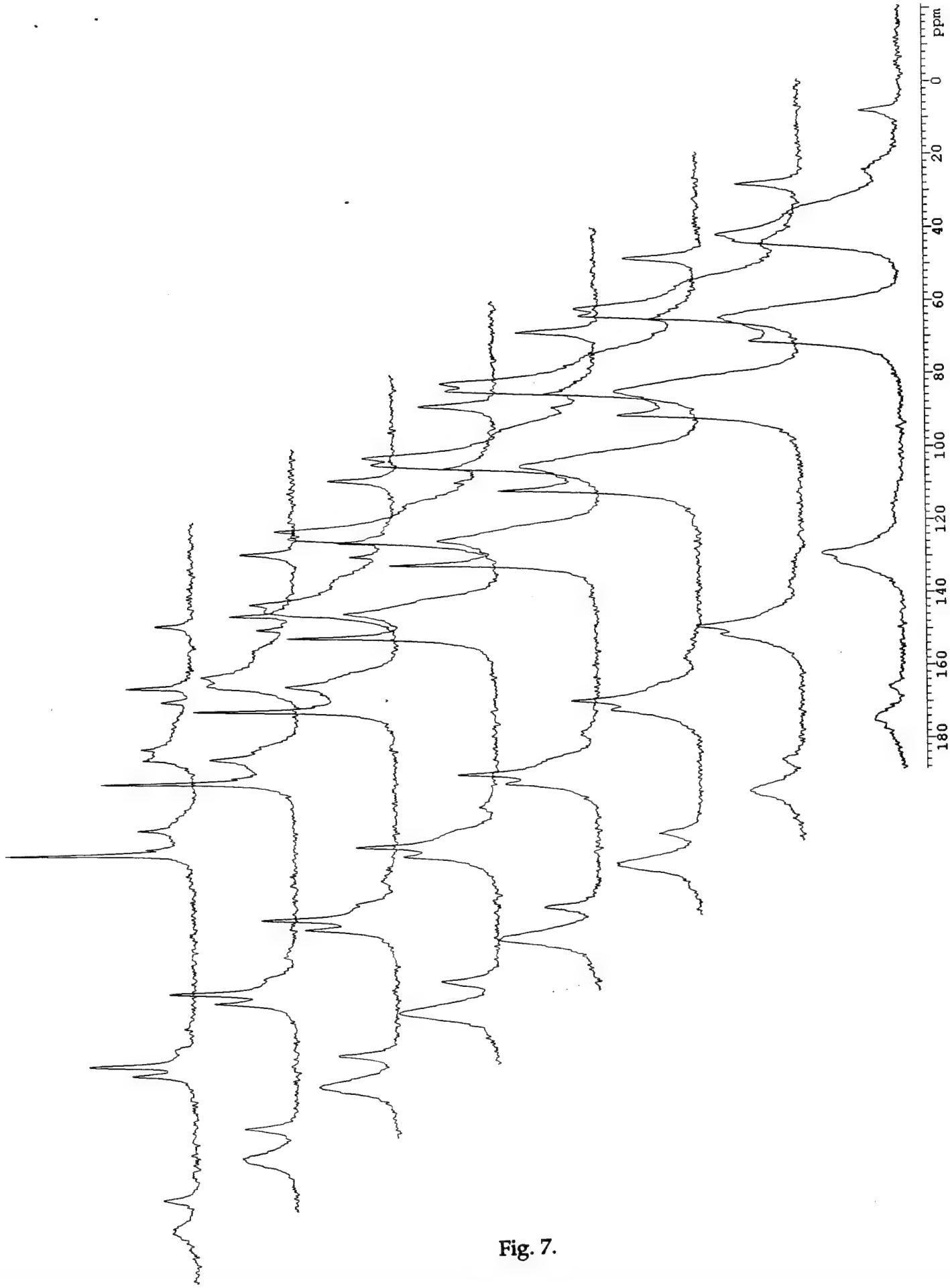

Fig. 7.

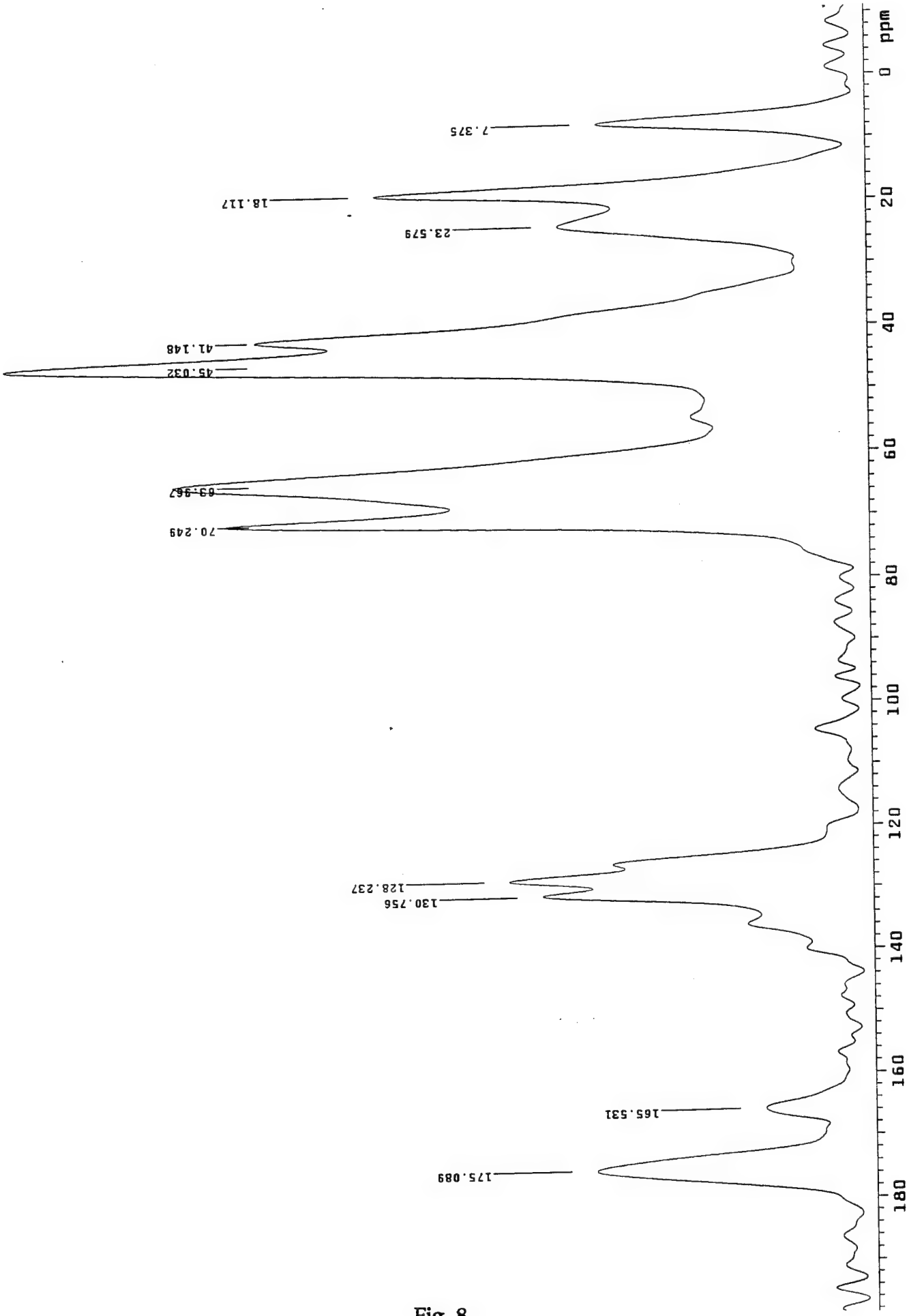
175.089
165.531
130.756
128.237
70.249
63.967
45.032
41.148
23.579
18.117
7.375
ppm
0
20
40
60
80
100
120
140
160
180

Fig. 8.

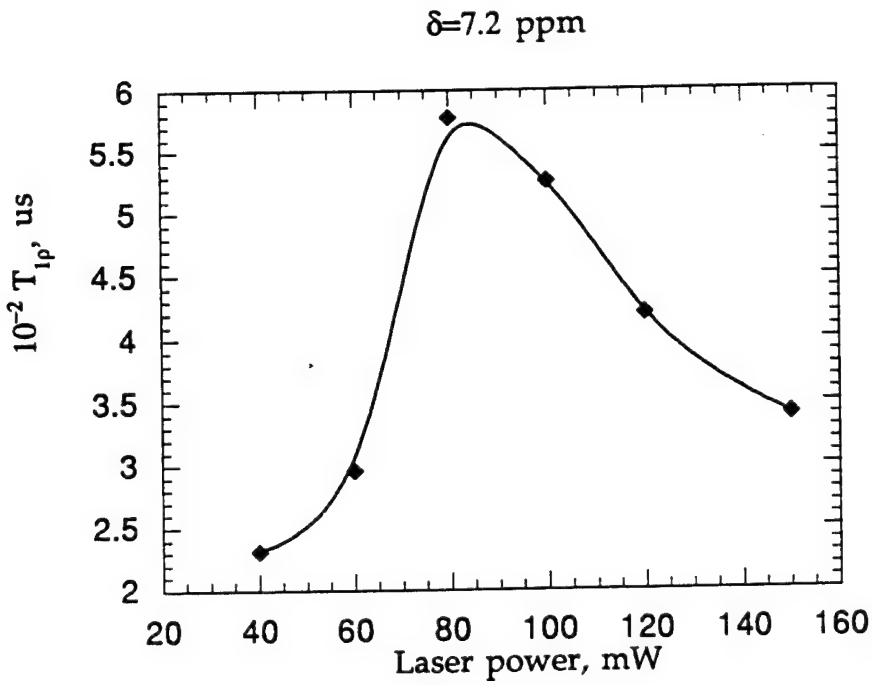
δ=7.2 ppm
6
5.5
5
4.5
4
3.5
3
2.5
2
10^{-2} $T_{1\rho}$, us
20
40
60
80
100
120
140
160
Laser power, mW

Fig. 9a.

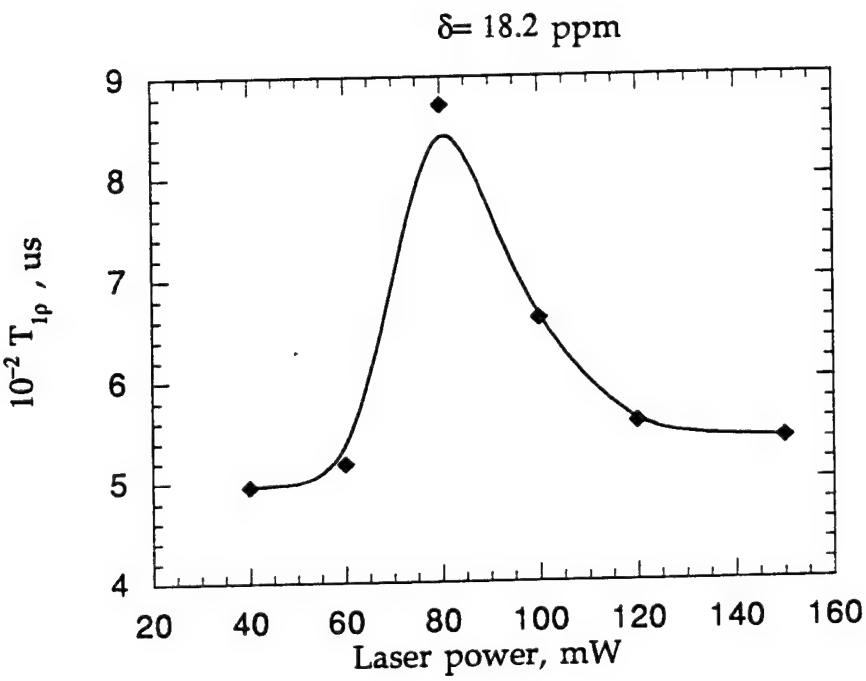
δ= 18.2 ppm
9
8
7
6
5
4
10^{-2} $T_{1\rho}$, us
20
40
60
80
100
120
140
160
Laser power, mW

Fig. 9b.

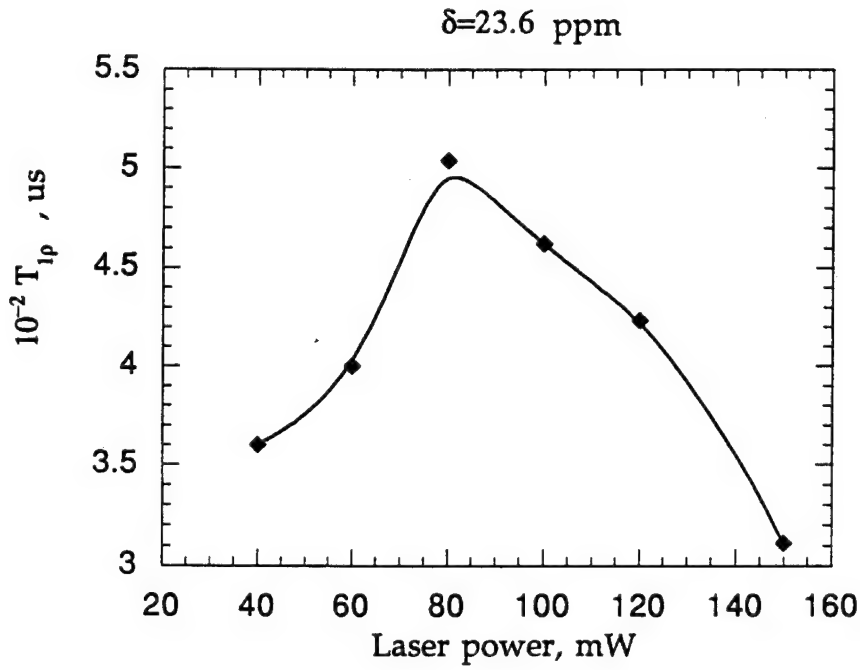
δ=23.6 ppm
5.5
5
4.5
4
3.5
3
10^{-2} $T_{1\rho}$, us
20
40
60
80
100
120
140
160
Laser power, mW

Fig. 9c.

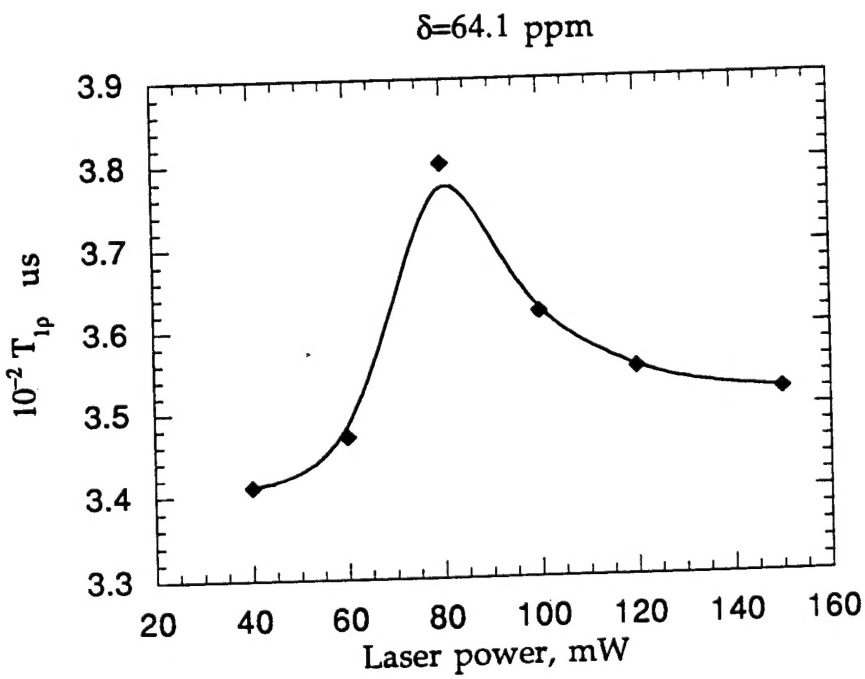
δ=64.1 ppm
3.9
3.8
3.7
3.6
3.5
3.4
3.3
10^{-2} $T_{1\rho}$ us
20
40
60
80
100
120
140
160
Laser power, mW

Fig. 9d.

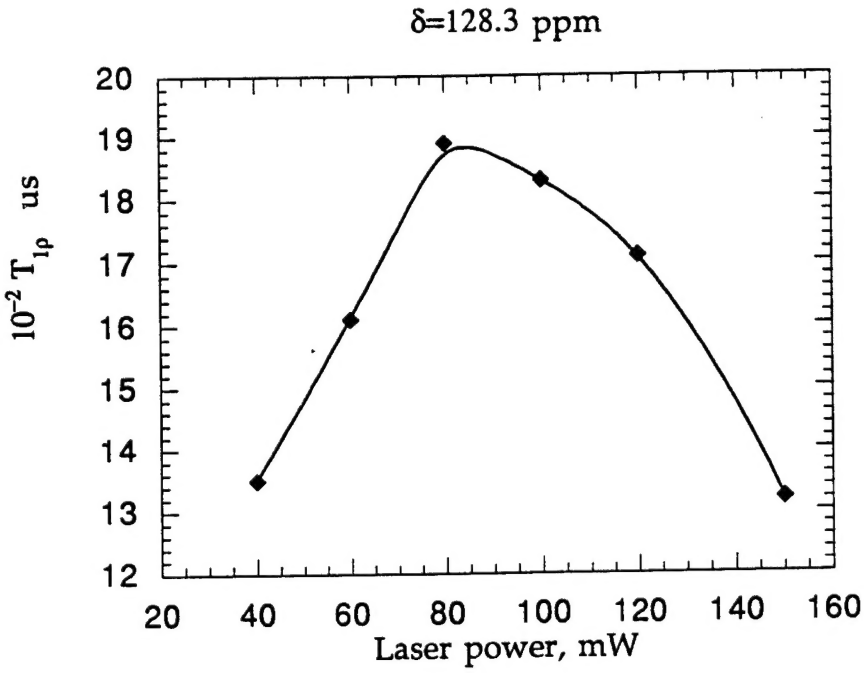
δ=128.3 ppm
20
19
18
17
16
15
14
13
12
10^{-2} $T_{1\rho}$ us
20
40
60
80
100
120
140
160
Laser power, mW

Fig. 9e

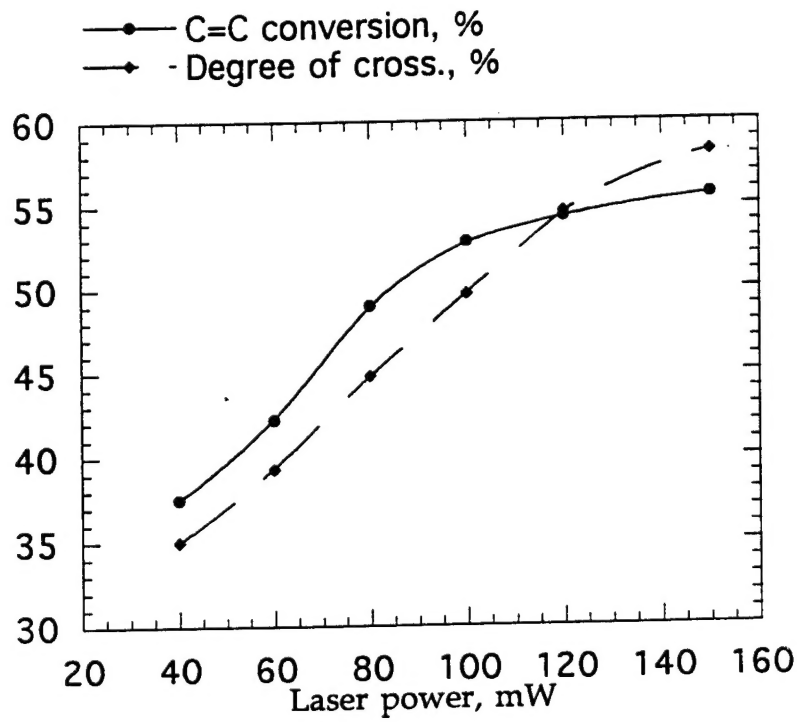
C=C conversion, %
Degree of cross., %
60
55
50
45
40
35
30
20
40
60
80
100
120
140
160
Laser power, mW

Fig. 10.

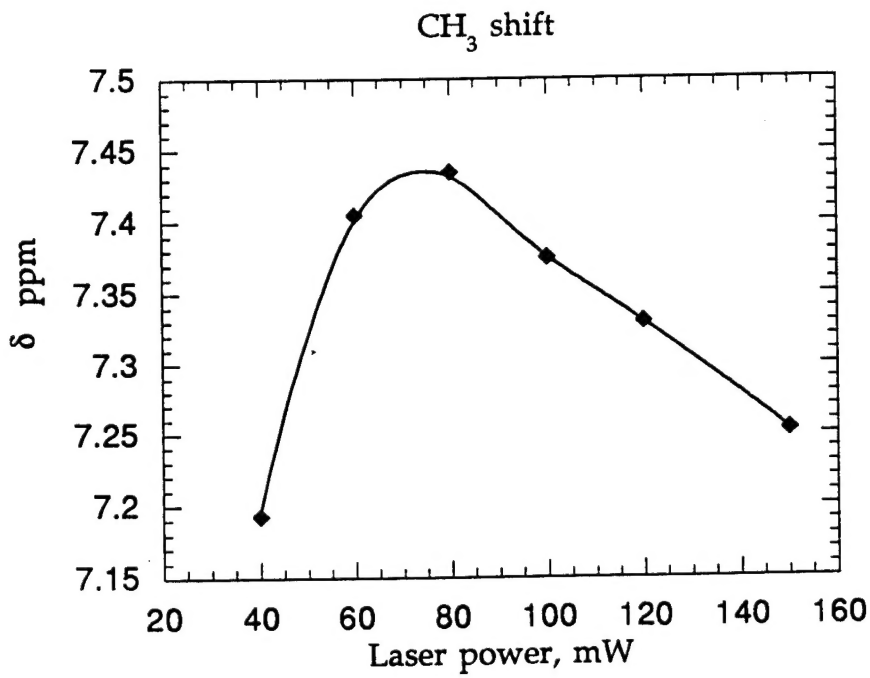
CH3 shift
7.5
7.45
7.4
7.35
7.3
7.25
7.2
7.15
δ ppm
20
40
60
80
100
120
140
160
Laser power, mW

Fig. 11.